

# Vehicle Reidentification With Self-Adaptive Time Windows for Real-Time Travel Time Estimation

Jiankai Wang, Nakorn Indra-Payoong, Agachai Sumalee, and Sakda Panwai

**Abstract**—This paper proposes a vehicle reidentification (VRI) system with self-adaptive time windows to estimate the mean travel time for each time period on the freeway under traffic demand and supply uncertainty. To capture the traffic dynamics in real-time application, interperiod adjusting based on the exponential smoothing technique is introduced to define an appropriate time-window constraint for the VRI system. In addition, an intraperiod adjusting technique is also employed to handle the non-predictable traffic congestion. To further reduce the negative effect caused by the mismatches, a postprocessing technique, including thresholding and stratified sampling, is performed on the travel time data derived from the VRI system. Several representative tests are carried out to evaluate the performance of the proposed VRI against potential changes in traffic conditions, e.g., recurrent traffic congestion, freeway bottlenecks, and traffic incidents. The results show that this method can perform well under traffic demand and supply uncertainty.

**Index Terms**—Stratified sampling, time window, travel time estimation, vehicle reidentification (VRI), video image processing (VIP) systems.

## I. INTRODUCTION

AS ONE of the best indicators for evaluation of the performance of the traffic system, accurate travel time data are crucial for efficient traffic management and transport planning. In addition, the individual travelers also require such information (e.g., mean travel time) to make a better route decision for their journeys. Therefore, it is of great importance to estimate the mean travel time in a robust and accurate manner. Because of the worldwide deployment of inductive loops, a large number of studies focused on utilizing the traffic data (e.g., spot speed and traffic flow) obtained from the traditional sensors to indirectly measure the mean travel time [1]–[3]. Despite their computational efficiency and analytical simplicity, these indirect methods based on traditional sensors would result in large errors when it comes to serious traffic congestion

[4], [5]. To overcome this difficulty, considerable attention has been paid to using the emerging sensing technologies to directly track the individual probe vehicle and, hence, collect the associated travel time (which could be termed as the probe-vehicle-based method). Various advanced technologies, such as Bluetooth [6], Global Positioning System technologies [7], license plate recognition technique [8], and cellular phones [9], have been incorporated to assign a unique identity (e.g., plate number, media access control address, and radio frequency identification tag) to the probe vehicle. By accurate matching of vehicle identities, the travel time of the probe vehicle can be directly measured. Although these probe-vehicle-based approaches appear promising for travel time estimation, their successes rely on a high penetration rate of probe vehicles. In addition, vehicle tracking based on the unique identity could raise privacy concerns. In this case, the vehicle reidentification (VRI) scheme, which does not intrude the driver's privacy, provides an alternative way to measure travel time.

Generally, VRI is a process of matching vehicle signatures (e.g., waveform [10], vehicle length [11], [12], vehicle color [13], [14], and partial plate number [15], [16]) from one detector to the next in the traffic network. On one hand, the nonuniqueness of the vehicle signature would allow the VRI system to track the vehicle anonymously. Moreover, the penetration rate is 100% in principle as no in-vehicle equipment is required. On the other hand, this property of very nonuniqueness imposes a great challenge on the development of the vehicle signature matching method. To improve the matching accuracy, Coifman [17] compared the lengths of vehicle platoons (i.e., vehicle platoon matching method). To further consider the noise and the nonuniqueness of the vehicle signature, Kwong *et al.* [18], [19] proposed a statistical matching method in which the vehicle signature is treated as a random variable, and a probabilistic measure is introduced for matching decision-making. The aforementioned approaches, however, are limited to the case with only one lane arterial and have a set of stringent assumptions on vehicle traveling behaviors (e.g., no overtaking and no lane changing). Sumalee *et al.* [20] extended the statistical signature matching method illustrated by Kwong *et al.* [18] to a more practical case in which overtaking between vehicles and vehicle matching across multiple lanes are both allowed. This proposed VRI system, which is also referred to as the basic VRI, is based on the emerging video image processing (VIP) systems [21], which enjoy several advantages over other traffic detectors (e.g., inductive loops and magnetic sensors) [22] as follows.

- First, VIP systems are capable of monitoring multiple lanes and can function as zone detectors rather than point sensors (e.g., magnetic sensor and inductive loops).

Manuscript received April 13, 2013; revised July 18, 2013; accepted September 2, 2013. Date of publication October 25, 2013; date of current version March 28, 2014. This work was supported by the Hong Kong Research Grants Council under General Research Fund PolyU 5242/12E. This work is also part of a collaborative research with the Division of Research and Development of Expressway Authority of Thailand. The Associate Editor for this paper was W.-H. Lin. (Corresponding author: A. Sumalee.)

J. Wang and A. Sumalee are with the Department of Civil and Environmental Engineering, The Hong Kong Polytechnic University, Kowloon, Hong Kong (e-mail: wjknju@gmail.com; ceasumalee@polyu.edu.hk).

N. Indra-Payoong is with the Department of Logistics and Supply Chain Management, Burapha University, Bangkok 10131, Thailand (e-mail: nakorn.ii@gmail.com).

S. Panwai is with the Expressway Authority of Thailand (EXAT), Bangkok 10900, Thailand (e-mail: sakda.duk@gmail.com).

Color versions of one or more of the figures in this paper are available online at <http://ieeexplore.ieee.org>.

Digital Object Identifier 10.1109/TITS.2013.2282163

- Unlike the inductive loops, VIP systems could provide us the speed-independent signature. Various detailed vehicle features (e.g., vehicle color, length, and type), which are independent of the vehicle speed, can be extracted.

A probabilistic data fusion rule was then introduced to combine these features derived from VIP systems to generate a matching probability (*posterior* probability) for matching decision-making. Sumalee *et al.* [20] also introduced a *prior* (fixed) time window, which sets the upper and lower bounds of the travel time in the hope of ruling out the unlikely candidate vehicles and, hence, improving the matching accuracy, which, in turn, would yield a more reliable travel time estimator. However, it is noteworthy that this basic VRI was specifically designed for a short time period in which the traffic condition is relatively stable (i.e., steady-state condition) and may not be applicable for “real time” application.

The development of the VRI system for “real time” implementation is still difficult as it faces the following two major challenges. First, due to the traffic demand and supply uncertainty (e.g., fluctuation in travel demand, bottleneck effect, and traffic incidents), the traffic condition may substantially change from period to period (i.e., free flow to congested). Under these circumstances, the fixed time-window constraint may compromise the performance of the basic VRI system. Thus, instead of explicitly incorporating the time window, Lin and Tong [23] utilized the travel time information estimated from the spot speed data and proposed a combined estimation model to reidentify the vehicles. As previously discussed that the travel time estimated from spot speed data is not reliable, this approach may not perform well under demand and supply uncertainty. Second, vehicle mismatches, which are caused by the nonuniqueness of the vehicle signature and the complex topological structure of the traffic network, are to be expected. This situation could be worse when a traffic incident happens. Therefore, a robust postprocessing technique regarding the individual travel time obtained from the VRI system is required. Ndoye *et al.* [24] suggested a data clustering method to filter out the erroneous individual travel time caused by the mismatches. For practical implementation, however, it may still be difficult to distinguish between the correct and erroneous travel time under “abnormal” traffic conditions (e.g., the occurrence of an incident or the bottleneck effect).

To this end, the objective of this paper is to propose an improved VRI system to cope with the real-time travel time estimation purpose. Specifically, this study aims to estimate the mean travel time for each time period (e.g., 5-min period) on the freeway under traffic demand and supply uncertainty. The proposed VRI system is based on authors’ previous work [20] with two major improvements as follows.

- First, to filter out the erroneous travel time caused by the mismatches, a thresholding process based on the matching probability is performed. A stratified sampling technique based on the vehicle type is then introduced to reduce the bias in the mean travel time estimates.
- Second, a self-adaptive time-window component (i.e., interperiod and intraperiod adjusting) is introduced into the basic VRI system to improve its robustness against po-

tential changes in traffic conditions. Interperiod adjusting of the time window based on the exponential smoothing technique is adopted to capture the traffic dynamics from period to period, whereas intraperiod adjusting is employed to handle the nonpredictable traffic congestion (e.g., caused by traffic incidents or the bottleneck effect).

After the theoretical development, various numerical tests are conducted to demonstrate the application of the improved VRI system. The first simulation test investigates the feasibility of utilizing the improved VRI system to estimate the mean travel time for a closed freeway segment containing recurrent congestion due to exceeding traffic demand. In the second simulation, the method is evaluated on a freeway corridor with on- and off-ramps. A freeway bottleneck then arises due to the high merging demand and lane drops. The simulation results show that the proposed method performs well under the bottleneck effect. The third simulation test is then conducted to test the performance of the algorithm under nonrecurrent congestion (caused by traffic incidents).

The rest of this paper is organized as follows: Section II presents a brief review on the basic VRI system. In Section III, the postprocessing technique (e.g., thresholding and stratified sampling) regarding the individual travel time obtained from the VRI system is introduced. The detailed description and analysis of the self-adaptive time-window component is proposed in the following section. In Section V, simulated tests are carried out to evaluate the performance of the proposed system. Finally, we close this paper with the conclusions and future works.

## II. BASIC VISION-BASED VRI SYSTEM

The basic vision-based VRI with a fixed time window is devised to estimate the mean travel time under static traffic conditions (e.g., a steady state of free flow/congestion). In line with the other traditional VRI schemes, the basic vision-based VRI also involves two major steps: 1) vehicle feature extraction; 2) vehicle signature matching method.

### A. Vehicle Feature Extraction

As the detailed traffic data (particularly the vehicle feature data) are not readily obtainable from the raw video record, various VIP techniques are then employed for extracting the required information.

1) *Vehicle Detection*: The success of vehicle detection largely depends on the degree that a moving object (vehicle) can be distinguished from its surroundings (background). In light of this, background estimation technology is employed in the detection subsystem. By calculating the media of a sequence of video frames, the background of the video image is obtained. Then, the image segmentation technique is performed to identify the foreground object (vehicle). The still image including the detected vehicle is then clipped and stored for further feature extraction. Along with the detection of the vehicle, the associated arrival time  $t$  and spot speed  $v$  are also collected. The normalized height of the vehicle image is adopted for representing vehicle length  $L$ .

2) *Vehicle Color Recognition*: Color is one of the most essential features for characterizing a vehicle. To reduce the negative effect of illumination changes, hue–saturation–value (HSV) color space is adopted to represent the vehicle image. First, the general RGB color images are converted into HSV color model-based images. Hue and saturation values are then exploited for color detection, whereas V (value) information is separated out from the color space. Second, a 2-D color histogram  $C$  is formed to represent the distribution (frequency) of colors across a vehicle image. To be more specific, the hue and saturation channels are divided into 36 and 10 bins, respectively. Thus, a color feature vector  $C$  with 360 elements is obtained.

3) *Vehicle Type Recognition*: The vehicle type feature provides other important information to describe a vehicle. In this research, the template matching method [25] is utilized to recognize vehicle type. This method uses the  $L_2$  distance metric to measure the similarity between the vehicle image and template images. Specifically, vehicles are classified into six categories. For each category, the corresponding template image is built for each lane. Finally, the normalized similarity value between the vehicle image ( $I$ ) and the  $k$ th template image ( $T$ ) is given by

$$S(k) = \frac{\sum_{m=1}^{\mathcal{M}} \sum_{n=1}^{\mathcal{N}} |I(m, n) - T(m, n)|^2}{\mathcal{G}\mathcal{M}\mathcal{N}} \quad (1)$$

where  $\mathcal{G}$  denotes the maximum gray level (255);  $\mathcal{M}$  and  $\mathcal{N}$  are the dimensions of the vehicle image. Thus, the vehicle type/shape feature  $S$  is a 6-D vector that consists of the similarity score for each template.

In other words, a vehicle signature, i.e.,  $X = \{C, S, L\}$ , is generated for each detected vehicle, where  $C$  and  $S$  are the normalized feature vector and the type (shape) feature vector, respectively;  $L$  denotes the vehicle length. As previously mentioned, the associated arrival time  $t$  and spot speed  $v$  are also obtained during the detection process. Therefore, the individual vehicle record can then be represented as  $(t, v, X)$ .

## B. Vehicle Signature Matching Method

For practical implementation, the vehicle records detected at the upstream station will be stored in the upstream database. Let  $U_i = (t_i^U, v_i^U, X_i^U)$  denote the record of the  $i$ th upstream vehicle, where  $X_i^U = \{C_i^U, S_i^U, L_i^U\}$  represents the associated vehicle signatures (i.e., color, type, and length). In this case, the upstream database is denoted as  $U = \{U_i | i = 1, 2, \dots\}$ , which could be updated with time propagation. Let  $D = \{D_j | D_j = (t_j^D, v_j^D, X_j^D), j = 1, 2, \dots, M\}$  denote the  $M$  vehicle records generated at the downstream station during a specific time period (e.g., 5-min period). The VRI is to find the corresponding upstream vehicles for these  $M$  downstream vehicles based on the generated vehicle signatures.

In order to quantify the difference between each pair of upstream and downstream vehicle signatures, several distance measures are then incorporated. Specifically, for a pair of sig-

natures  $(X_i^U, X_j^D)$ , the Bhattacharyya distance [26] is utilized to calculate the degree of similarity between color features, i.e.,

$$d_{\text{color}}(i, j) = \left[ 1 - \sum_{k=1}^{360} \sqrt{C_i^U(k) \cdot C_j^D(k)} \right]^{1/2} \quad (2)$$

where  $k$  denotes the  $k$ th component of the color feature vector. The  $L_1$  distance measure is introduced to represent the difference between the type feature vectors, i.e.,

$$d_{\text{type}}(i, j) = \sum_{k=1}^6 |S_i^U(k) - S_i^D(k)|. \quad (3)$$

The length difference is given by

$$d_{\text{length}}(i, j) = |L_i^U - L_j^D|. \quad (4)$$

However, in practice, it is unnecessary to compute the distance between all pairs of upstream and downstream vehicle signatures. To rule out the unlikely candidate vehicles at the upstream database and improve the overall computational efficiency, a time-window constraint is introduced.

1) *Time-Window Constraint*: A time window, which sets the upper and lower bounds of travel time, is introduced to define the search space (i.e., set of potential upstream matches) for the downstream vehicle. Given a downstream vehicle  $j \in \{1, 2, \dots, M\}$ , its search space, i.e.,  $\mathcal{S}(j)$ , is given by

$$\mathcal{S}(j) = \{i | t_j^D - t_{\max} \leq t_i^U \leq t_j^D - t_{\min}\} \quad (5)$$

where  $t_{\max}$  and  $t_{\min}$  are, respectively, the upper and lower bounds of the time window. For a sequence of downstream vehicles  $\{1, 2, \dots, M\}$ , the set of the candidate upstream vehicles, i.e.,  $\mathcal{S}$ , is defined as

$$\mathcal{S} = \bigcup_{j=1}^M \mathcal{S}(j). \quad (6)$$

Under the static traffic condition, the time window  $[t_{\min}, t_{\max}]$  can be calibrated from the available historical travel time data.

With the associated search space  $\mathcal{S}$ , the vehicle signature matching method is equivalent to finding the correspondence between  $\{1, 2, \dots, M\}$  and  $\mathcal{S}$ . Herein we introduce an indicator variable to represent the matching result, i.e.,

$$x_{ij} = \begin{cases} 1, & \text{downstream vehicle } j \text{ matches} \\ & \text{upstream vehicle } i \in \mathcal{S} \\ 0, & \text{otherwise.} \end{cases} \quad (7)$$

Recall that for each pair of vehicle signatures,  $(X_i^U, X_j^D)$ ,  $i \in \mathcal{S}$ ,  $j \in \{1, 2, \dots, M\}$ , one may compute the distance  $(d_{\text{color}}(i, j), d_{\text{type}}(i, j), d_{\text{length}}(i, j))$  based on (2)–(4). A simple solution (i.e., distance-based method) is then to find the matching result  $x_{ij}$  with the minimum feature distance. However, it should be noted that the vehicle signatures contain potential noise and are not unique. Therefore, the distance measure cannot really reflect the similarities between the vehicles. Instead of directly comparing the feature distances, this study utilizes the statistical matching method. Based on the calculated

feature distance ( $d_{\text{color}}(i, j)$ ,  $d_{\text{type}}(i, j)$ ,  $d_{\text{length}}(i, j)$ ), a matching probability  $P(x_{ij} = 1 | d_{\text{color}}, d_{\text{type}}, d_{\text{length}})$  is provided for the matching decision-making.

2) *Calculation of Matching Probability*: The matching probability, which is also referred to as the *posterior* probability, plays a fundamental role in the proposed VRI system. By applying the Bayesian rule, one may have

$$P(x_{ij} = 1 | d_{\text{color}}, d_{\text{type}}, d_{\text{length}}) = \frac{p(d_{\text{color}}, d_{\text{type}}, d_{\text{length}} | x_{ij} = 1) P(x_{ij} = 1)}{p(d_{\text{color}}, d_{\text{type}}, d_{\text{length}})} \quad (8)$$

where  $p(d_{\text{color}}, d_{\text{type}}, d_{\text{length}} | x_{ij} = 1)$  is the likelihood function;  $P(x_{ij} = 1)$  is the prior knowledge about the matching result without observing the detailed vehicle feature data. In addition, one may also have

$$p(d_{\text{color}}, d_{\text{type}}, d_{\text{length}}) = p(d_{\text{color}}, d_{\text{type}}, d_{\text{length}} | x_{ij} = 1) P(x_{ij} = 1) + p(d_{\text{color}}, d_{\text{type}}, d_{\text{length}} | x_{ij} = 0) P(x_{ij} = 0). \quad (9)$$

Based on (8) and (9), it is observed that the calculation of the matching probability is dependent on the deduction of the likelihood function and the prior probability. In this particular case, the prior probability is approximated by the historical travel time distribution, i.e.,

$$P(x_{ij} = 1) = \frac{f(t(i, j))}{\eta} \times 0.5 \quad (10)$$

$$P(x_{ij} = 0) = 1 - \frac{f(t(i, j))}{\eta} \times 0.5 \quad (11)$$

where  $f(\cdot)$  denotes the historical travel time distribution,  $t(i, j)$  is the time difference between upstream vehicle  $i$  and downstream vehicle  $j$ , and  $\eta$  is the normalizing factor.

The calculation of the likelihood function is completed in two steps. First, individual statistical models for the three feature distances are constructed, and the corresponding likelihood functions are also obtained (i.e.,  $p(d_{\text{color}} | x_{ij} = 1)$ ,  $p(d_{\text{type}} | x_{ij} = 1)$ , and  $p(d_{\text{length}} | x_{ij} = 1)$ ). Then, a data fusion rule is employed to provide an overall likelihood function used in *posterior* probability (8).

3) *Statistical Modeling of Feature Distance*: Without loss of generality, only the probabilistic modeling of color feature distance is described. In the framework of statistical modeling, the distance measure is assumed to be a random variable. Thus, for a pair of color feature vectors ( $C_i^U, C_j^D$ ), the distance  $d_{\text{color}}(i, j)$  follows a certain statistical distribution. The conditional probability (i.e., likelihood function) of  $d_{\text{color}}(i, j)$  is then given by

$$p(d_{\text{color}}(i, j) | x_{ij}) = \begin{cases} p_1(d_{\text{color}}(i, j)), & \text{if } x_{ij} = 1 \\ p_2(d_{\text{color}}(i, j)), & \text{if } x_{ij} = 0 \end{cases} \quad (12)$$

where  $p_1$  denotes the probability density function (pdf) of distance  $d_{\text{color}}(i, j)$  when color feature vectors  $C_i^U$  and  $C_j^D$  belong to the same vehicle, whereas  $p_2$  is the pdf of the distance  $d_{\text{color}}(i, j)$  between different vehicles. A historical training

data set that contains a number of pairs of correctly matched vehicles are utilized for estimating pdfs  $p_1$  and  $p_2$ . Likewise, the likelihood functions for the type and length distances can be also obtained in a similar manner.

4) *Data Fusion Rule*: In this paper, the logarithmic opinion pool (LOP) approach is employed to fuse the individual likelihood functions. The LOP is evaluated as a weighted product of the probabilities, and the equation is given by

$$p(d_{\text{color}}, d_{\text{type}}, d_{\text{length}} | x_{ij}) = \frac{1}{Z_{\text{LOP}}} p(d_{\text{color}} | x_{ij})^\alpha p(d_{\text{type}} | x_{ij})^\beta p(d_{\text{length}} | x_{ij})^\gamma, \quad \alpha + \beta + \gamma = 1 \quad (13)$$

where fusion weights  $\alpha$ ,  $\beta$ , and  $\gamma$  are used to indicate the degree of contribution of each likelihood function, and  $Z_{\text{LOP}}$  is the normalizing constant. The weights can be also calibrated from the training data set. By substituting (9), (10), and (13) into (8), the desired matching probability can be obtained. For the sake of simplicity, let  $P_{ij}$  denote the matching probability between upstream vehicle  $i \in \mathcal{S}$  and downstream vehicle  $j$ .

5) *Bipartite Matching Method*: Recall that the basic VRI system is to find the matching result  $x_{ij}$  between the downstream vehicle set  $\{1, 2, \dots, M\}$  and its search space  $\mathcal{S}$  (assume that there are  $N$  candidate vehicles) simultaneously based on matching probability  $\{P_{ij} | i = 1, 2, \dots, N; j = 1, 2, \dots, M\}$ . The signature matching problem is then formulated as

$$\min_x \sum_{i=1}^N \sum_{j=1}^M -P_{ij} x_{ij} \quad (14)$$

$$\text{s.t. } x_{ij} \in \{0, 1\}, \quad \forall i \in \mathcal{S}, j \in \{1, 2, \dots, M\} \quad (15)$$

$$\sum_{i=1}^N x_{ij} = 1, \quad \forall j \in \{1, 2, \dots, M\} \quad (16)$$

$$\sum_{j=1}^M x_{ij} \leq 1, \quad \forall i \in \mathcal{S}. \quad (17)$$

Objective (14) is to maximize the overall matching probabilities between the two sets. Constraint (15) ensures that the decision variables are binary integers. Constraint (16) requires that a downstream vehicle can have one matched vehicle at the upstream station, whereas constraint (17) guarantees that an upstream vehicle can have, at most, one matched vehicle at downstream (normally  $N > M$ ). This combinatorial optimization problem is equivalent to a minimum-weight bipartite matching problem, which has already been widely studied and can be efficiently solved by the successive shortest path algorithm with computational complexity of  $O(M^2N)$ .

6) *Discussion on the Application of the Basic VRI System*: The detailed implementation of the basic VRI for mean travel time estimation (e.g., from 10:00 A.M. to 10:05 A.M.) is summarized in the following flowchart (see Fig. 1). First, the system will initialize time stamp  $t$  and check whether a vehicle is detected at the upstream and/or downstream stations. The

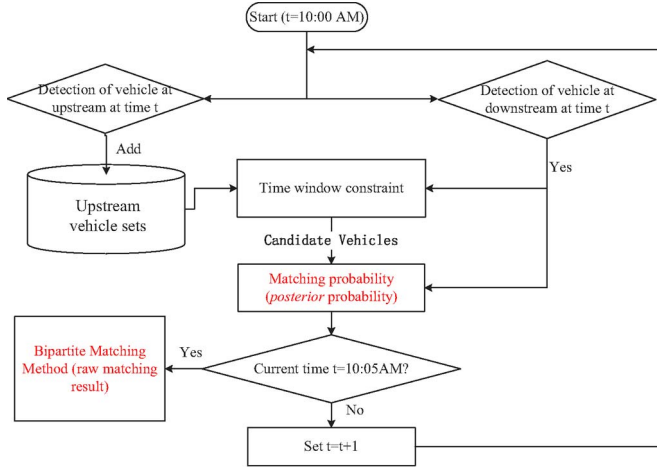


Fig. 1. Illustrative example of the basic VRI system.

generated upstream vehicle records are stored in the upstream vehicle database. Once a vehicle is detected at the downstream station, the candidate vehicle set will be selected based on the time-window constraint. Meanwhile, the matching probability for each pair of vehicles is calculated. When current time  $t$  reaches 10:05 A.M., the bipartite matching process based on the matching probability will begin, and the travel time data can be obtained. A detailed implementation of this system can be found in [20]. For the aforementioned framework, the following four comments should be taken into account.

- First, it is noteworthy that the calculation of the matching probability can be simultaneously performed along with the vehicle detection process at the downstream site (i.e., during the 5-min time period). In addition, the bipartite matching process can be carried out efficiently as explained before. Thus, the basic VRI can be implemented in real time (which will be explained in detail in Section V-A).
- Second, it is observed that the basic VRI heavily depends on the specification of the time window. When a large time window is applied, search space  $\mathcal{S}$  would include too many candidate vehicles, which could lead to a significant increase in computational time. On the other hand, a relatively smaller time window may enable the algorithm to find the corresponding vehicle more efficiently; however, it may also wrongly exclude the correct match from search space  $\mathcal{S}$ .
- Third, by using the historical travel time distribution to approximate the prior knowledge ( $P(x_{ij} = 1)$ ), one may obtain a more reliable matching probability. In other words, the basic VRI accepts the predefined time window and the historical travel time distribution as exogenous inputs and then perform the vehicle matching method. Both of these two inputs can be derived from the mean travel time data (which will be explained in Section IV).
- Fourth, the basic VRI cannot work well under traffic demand and supply uncertainty, as the time window and prior knowledge may not be well defined. From the perspective of mean travel time estimation, two novel components

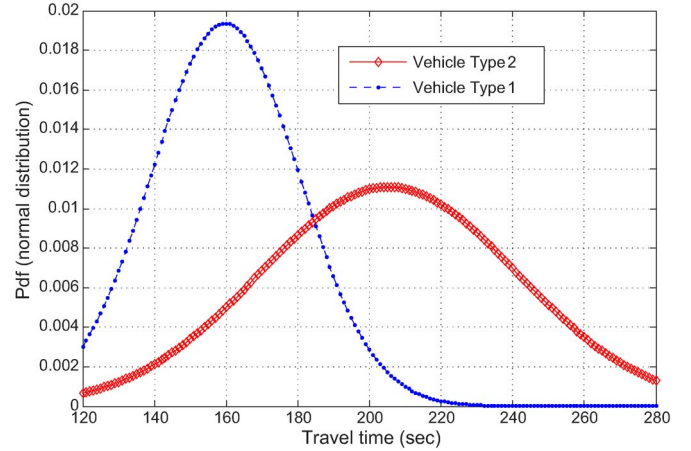


Fig. 2. Travel time for different vehicle types.

(i.e., postprocessing and self-adaptive time window) can be incorporated to improve the overall performance.

### III. POSTPROCESSING TECHNIQUE

Upon completion of the basic VRI system, the raw travel time for the  $j$ th,  $j \in \{1, 2, \dots, M\}$  downstream vehicle during the evaluation period can be obtained and denoted as  $t_j^r$ . Thus, the mean travel time without postprocessing is given by

$$\mu^r = \frac{1}{M} \sum_{j=1}^M t_j^r. \quad (18)$$

As the mismatches due to the nonuniqueness of the vehicle signature are inevitable, the raw travel time may include erroneous information. Hence, accordingly, the estimator  $\mu^r$  may not be reliable in practice.

#### A. Stratified Sampling Technique

One natural method is to perform thresholding on the raw travel time data based on the associated matching probability in an attempt to rule out the mismatches. However, another problem (i.e., biased estimation) may arise along with this thresholding process. It is commonly believed that the travel time of vehicles of different types (e.g., small cars and long trucks) is significantly different. Fig. 2 shows the travel time of different vehicle types fitted by a normal distribution, where vehicle type 1 denotes smaller cars, and vehicle type 2 represents long trucks. These ground truth travel time data are collected from a freeway segment in Bangkok, Thailand. The authors also conducted various hypothesis tests (i.e.,  $t$ -tests) to validate this assumption. Thus

$$H_0 : \mu_{\text{type1}} = \mu_{\text{type2}} \quad \text{vs.} \quad H_\alpha : \mu_{\text{type1}} \neq \mu_{\text{type2}}$$

where  $\mu_{\text{type1}}$  and  $\mu_{\text{type2}}$  are the mean travel time of small cars and long trucks, respectively. The results show that the null hypothesis should be rejected, which means that the travel times of different types of vehicles are “statistically” different. In view of this, to further reduce the bias in mean travel time estimation, the stratified sampling technique [27] based on the

vehicle type is proposed. Specifically, the raw travel time data  $\{t_j^r | j = 1, 2, \dots, M\}$  are divided into two strata (i.e., small-car stratum and long-truck stratum). The thresholding processes are independently performed on these two strata. The final mean travel time  $\mu$  is then computed as the weighted average of the mean travel time over all vehicle type strata. The equation is then given as

$$\mu = \sum_{k=1}^2 \frac{M_k}{M} \left( \frac{1}{n_k} \sum_{j=1}^{n_k} t_{jk} \right) \quad (19)$$

where  $M_k$  is the number of vehicles of type  $k$ ,  $n_k$  denotes the sample size of vehicles of type  $k$  after the thresholding process, and  $t_{jk}$  is the travel time of the  $j$ th vehicle of type  $k$  after the thresholding process. The design of the thresholding process becomes the major concern in the following section.

### B. Thresholding Process

For each individual vehicle stratum, the thresholding process is independently performed. As explained before, one of the outputs of basic VRI is the matching result  $x_{ij}$ , whereas the other output is the associated matching probability  $P_{ij}$ . The overall idea of thresholding is to apply a certain rule to these outputs (i.e.,  $x_{ij}$  and  $P_{ij}$ ) in order to identify the associated erroneous travel time.

For downstream vehicle  $j$  in vehicle stratum  $k$ , the matched upstream vehicle  $i^* = \{i \in \mathcal{S} | x_{ij} = 1\}$  and the associated matching probability is  $P_{i^*j}$ . One naive approach to rule out those mismatches would be to impose a threshold value on the matching probability. If  $P_{i^*j}$  is greater than the threshold value, then the travel time data regarding this vehicle  $j$  would be retained for the following stratified sampling [see (19)]. However, in practical implementation, we find that the single matching probability cannot really reflect the correctness of the matching. It is quite possible that the other matching probability  $P_{lj} \approx P_{i^*j}$ ,  $l \in \mathcal{S}; l \neq i^*$ , which means that the VRI system cannot distinguish between the candidate vehicles. To account for this problem, this study proposes a new measure to represent the distinctiveness of the vehicle. For this specific vehicle  $j$ , the distinctiveness value is defined as

$$\frac{P_{i^*j}}{P_j^{(2)}}, P_j^{(2)} \text{ is the second largest matching probability of } \{P_{ij} | \forall i \in \mathcal{S}\}. \quad (20)$$

Recall that the proposed bipartite matching method finds the matching result with the overall maximum probability [see (14)]. In this case, for a certain downstream vehicle, it may not be matched to the upstream vehicle with the maximum likelihood. Therefore, by calculating the distinctiveness value, one may get more information about the matching result, i.e.,

$$\frac{P_{i^*j}}{P_j^{(2)}} = \begin{cases} \geq 1, & \text{vehicle } j \text{ matches upstream vehicle with} \\ & \text{maximum probability} \\ = 1, & \text{vehicle } j \text{ matches upstream vehicle with} \\ & \text{the second largest probability} \\ < 1, & \text{vehicle } j \text{ matches the other ones.} \end{cases}$$

If vehicle  $j$  and upstream vehicle  $i^*$  are truly matches, then the ratio between  $P_{i^*j}$  and  $P_j^{(2)}$  is expected to be relatively larger. Based on this basic idea, a predefined threshold value  $\tau > 1$  is then imposed on this distinctiveness value, i.e.,

$$\begin{cases} P_{i^*j}/P_j^{(2)} > \tau, & \text{travel time } t_{jk} \text{ is retained for} \\ & \text{stratified sampling} \\ \text{Otherwise,} & \text{travel time } t_{jk} \text{ is discarded.} \end{cases} \quad (21)$$

By applying rule (21), the erroneous individual travel time data are expected to be identified and ruled out.

## IV. SELF-ADAPTIVE TIME-WINDOW CONSTRAINT

Although the basic VRI is improved to some extent by imposing the postprocessing technique on the raw travel time data (see Section III), it still cannot perform well under traffic demand and supply uncertainty. (Some preliminary results are presented in Section V.) As mentioned in Section II, the basic VRI heavily depends on the specification of two exogenous inputs, i.e., time window and prior knowledge. Therefore, to further improve the robustness of the VRI system against potential changes in traffic conditions, these two inputs should be adjusted accordingly (i.e., self-adaptive).

Intuitively, the time window can be derived from the travel time data (i.e., travel time distribution). Given the mean value  $\mu_t$  and the variance  $\sigma_t^2$  of the travel time distribution during time period  $t$ , a suitable time window  $[Lb_t, Ub_t]$  could be easily obtained. Assume that the travel time follows normal distribution  $N(\mu_t, \sigma_t)$ , then the tolerance interval with a 95% confidence level can be utilized to define the time window, i.e.,

$$[Lb_t, Ub_t] = [\mu_t - 1.96\sigma_t, \mu_t + 1.96\sigma_t]. \quad (22)$$

Given the coefficient of variation  $\phi$ , the time-window constraint can be rewritten as

$$[Lb_t, Ub_t] = [(1 - 1.96\phi)\mu_t, (1 + 1.96\phi)\mu_t]. \quad (23)$$

Moreover, the prior knowledge can be approximated by the normal distribution  $N(\mu_t, \phi\mu_t)$ . Therefore, both of these two critical inputs of basic VRI can be derived from the prediction of the mean travel time in time period  $t$ . In other words, the self-adjusting of the time window and the prior knowledge can be completed by iteratively predicting the mean travel time for each time period. In this research, the self-adjusting of the time window for real-time application involves two major steps as follows.

- Interperiod adjusting: Based on current traffic information (e.g., average spot speed) and the mean travel time value in a previous time period (i.e., obtained from the VRI system), one may predict the mean travel time value for the next time period (i.e., interperiod adjusting), from which the time window is derived. The exponential forecasting technique integrated with the average spot speed information is adopted during the interperiod adjusting process.
- Intraproduct adjusting: Since the nonrecurrent traffic congestion (e.g., caused by incidents) is not predictable, the additional intraproduct adjustment is required for providing

an appropriate time window under these extreme circumstances. An iterative bipartite matching method is proposed for adjusting the time window, in which the basic VRI is iteratively solved.

Note that the purpose of predicting the mean travel time is to derive an appropriate time window, and the accuracy of the prediction is not our major concern. As a matter of fact, the estimated mean travel time is obtained from the VRI system with the postprocessing technique.

### A. Interperiod Adjusting

We introduce time series theory for short-term travel time prediction. As a classical statistical approach, time series forecasting has already been evaluated with several other applications in transportation, such as short-term traffic flow prediction [28] and traffic speed forecasting [29].

In this paper, the underlying model equation for the mean travel time data is assumed as

$$\mu_t = \mu_t^* + \varepsilon_t \quad (24)$$

where  $\mu_t$  is the mean travel time calculated from the VRI system,  $\mu_t^*$  represents the ground truth data, and  $\varepsilon_t$  is the white noise error term. Our goal is to roughly forecast the mean travel time in period  $t + 1$  (i.e., short-term prediction). Therefore, the exponential smoothing technique integrated with spot speed information is employed for this particular purpose.

1) *Exponential Smoothing Technique*: The smoothing (forecasting) equation is given as

$$\tilde{\mu}_{t+1} = \tilde{\mu}_t + \varphi(\mu_t - \tilde{\mu}_t) \quad (25)$$

$$\tilde{\mu}_{t+1} = \frac{V_t^U + V_t^D}{V_{t+1}^U + V_{t+1}^D} \tilde{\mu}_{t+1} \quad (26)$$

where  $\tilde{\mu}_{t+1}$  and  $\tilde{\mu}_t$  denote the forecasters of the mean travel time in time period  $t + 1$  and period  $t$ , respectively;  $\varphi$  represents the smoothing parameter that is calibrated from the historical data;  $V_t^U$  and  $V_t^D$  are the average speed at upstream and downstream stations, respectively, during time period  $t$ ; and likewise,  $V_{t+1}^U$  and  $V_{t+1}^D$  are the average speed at upstream and downstream stations, respectively, during time period  $t + 1$ . Equation (25) serves as a simple exponential estimation based on the estimates from previous steps, whereas (26) is a correction step by utilizing the average spot speed. The rationale behind (26) is as follows. If the average spot speeds at both stations (i.e., upstream and downstream) decrease from period  $t$  to period  $t + 1$ , the mean travel time during time period  $t + 1$  is expected to be larger.

Following the prediction of  $\tilde{\mu}_{t+1}$ , the time window for period  $t + 1$  is given by

$$[Lb_{t+1}, Ub_{t+1}] = [(1 - 1.96\phi)\tilde{\mu}_{t+1}, (1 + 1.96\phi)\tilde{\mu}_{t+1}]. \quad (27)$$

Based on these recursive formulas, one may be able to predict the mean travel time and the time window from period to period (i.e., interperiod adjusting). However, it should be noted that a “bad” prediction could potentially lead to low matching

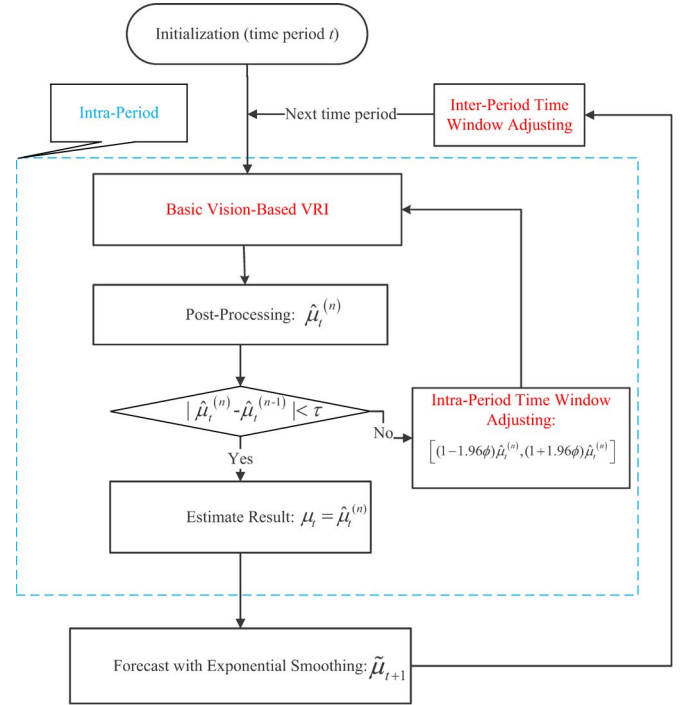


Fig. 3. Detailed implementation of the improved VRI system.

accuracy of the VRI system and, hence, unreliable travel time estimates. Thus, the additional intraperiod adjusting method should be developed.

### B. Intra-period Adjusting

From time period  $t + 1$ , the predicted time window  $[Lb_{t+1}, Ub_{t+1}]$  and  $\tilde{\mu}_{t+1}$  are derived during the interperiod adjusting process and then fed into the basic VRI system, from which the raw travel time data can be obtained. By performing the postprocessing technique (e.g., thresholding and stratified sampling), an improved mean travel time estimator, i.e.,  $\hat{\mu}_{t+1}^{(1)}$ , is then calculated. In practice, the initial prediction of the time window may not be reliable (particularly when an incident happens), which could significantly decrease the performance of the VRI system. Thus, it is expected that  $\hat{\mu}_{t+1}^{(1)}$  would not be accurate. In light of this, an iterative process is devised to solve the basic VRI problems iteratively with different exogenous inputs (i.e., time window and prior probability). To be more specific, a new time window, i.e.,  $[(1 - 1.96\phi)\hat{\mu}_{t+1}^{(1)}, (1 + 1.96\phi)\hat{\mu}_{t+1}^{(1)}]$ , is calculated based on the estimated mean travel time  $\hat{\mu}_{t+1}^{(1)}$ . Then, the basic VRI and the associated postprocessing technique are performed again using this new time window. This iterative process will continue until the relative change in the estimated mean travel time is sufficiently small. In this research, the error for stopping tolerance of the convergence is given by

$$\left| \hat{\mu}_{t+1}^{(n)} - \hat{\mu}_{t+1}^{(n-1)} \right| \leq \tau \quad (28)$$

where superscript  $n$  represents the iteration number, and  $\tau$  is the stopping tolerance (see Fig. 3).

To sum up, interperiod adjusting is designed to capture the traffic dynamics from period to period, whereas intraperiod

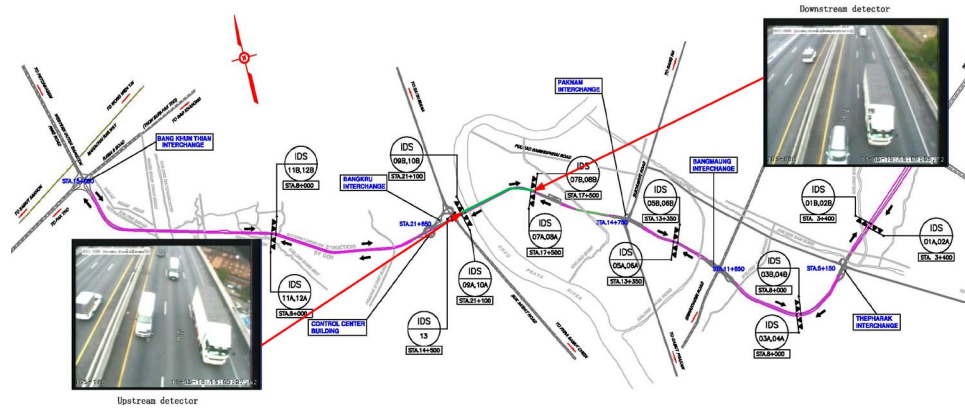


Fig. 4. Test site in Bangkok, Thailand.

adjusting (i.e., iterative process) is introduced to handle the nonpredictable traffic conditions (e.g., traffic incidents and bottleneck effect).

## V. EXPERIMENTAL RESULTS

To verify the effectiveness and feasibility of the proposed improved VRI system, various simulation-based experiments are conducted. In this research, a VISSIM-based simulation model is devised to simulate freeway system operations under traffic demand and supply uncertainty (e.g., free flow, congestion, bottleneck effect, and traffic incident).

### A. Simulation Model Configuration and Calibration

Before presenting the experimental results, the detailed procedures for simulation model development and calibration are introduced. The test site for this research is a 34.9-km-long three-lane freeway system in Bangkok, Thailand (see Fig. 4). At each station, a gantry-mounted video camera, which is viewed in the upstream direction, is installed, and the associated video records are collected. Two segments are chosen for simulation model development: 1) a 3.6-km-long closed segment (i.e., between 08A and 10A, the green section in Fig. 4); 2) a 4.2-km-long corridor with on/off-ramps (i.e., between 02A and 04A). The simulation model is then configured based on the exact roadway geometric feature, including the length of the segment, the location of on/off-ramps, and the number of lanes.

To guarantee realistic representations of the simulated experiments, model calibration is required. With the video records collected at the test site, the individual vehicles can be detected and manually reidentified across multiple stations. Accordingly, the ground truth data, such as vehicle counts, traffic demand, and travel time data, can be obtained for model calibration. The correctly matched pairs of vehicle images are stored in the image database for further application.

Upon completion of the simulation model configuration and calibration, the travel behavior and characteristic of each individual vehicle (e.g., speed, vehicle type, and arrival time at each station) can be collected. As the very heart of the proposed method is the vision-based VRI, a vehicle image, which is randomly selected from the image database, is assigned to the vehicle records generated from the simulation model. These

newly created vehicle records are then fed into the improved VRI system.

To sum up, we simulate all traffic conditions (recurrent and nonrecurrent traffic congestion) using VISSIM and implement the proposed method in MATLAB. To be more specific, the experiments are performed under Windows 7 Home Premium and MATLAB v7.14 (R2012a) running on a Dell desktop with an Intel(R) Core(TM) i3 CPU at 3.20 GHz and with 4.00 GB of memory. It is easily observed that the computational time of the proposed method largely depends on the number of intraperiod iteration steps and the CPU time of the basic VRI system (see Fig. 3). Some preliminary experiments also show that the average CPU time used by the bipartite matching method in basic VRI under the free-flow condition is 0.0896 s, whereas the average CPU time under the congested condition is about 0.3294 s. Therefore, it is reasonable to believe that the improved VRI system can be implemented for real-time application.

### B. Preliminary Comparison Between Basic VRI and Improved VRI

To conduct the comparison of the basic VRI and the improved VRI system, a VISSIM-based simulation model is designed for the closed segment between 08A and 10A (Westbound). During the 4-h simulation time period, approximately 16 000 pairs of vehicle records are generated. These vehicles can be roughly categorized into two types (see Section III): 70% of small cars and 30% of long vehicles. For this specific segment, the associated image database, which includes 6280 pairs of vehicle images, is built up. Therefore, a complete record for vehicle  $i$  can be denoted as  $(ID_i, t_i, v_i, X_i)$ , where  $ID_i$  is the unique identity derived from the simulation model;  $t_i$  and  $v_i$  are, respectively, the arrival time and spot speed of vehicle  $i$ ; and  $X_i$  represents vehicle feature data extracted from the vehicle image. Based on these simulation data, the proposed VRI system is performed and evaluated in terms of the matching accuracy and the effectiveness of mean travel time estimation.

For the closed freeway segment, each vehicle can be detected at both stations. Therefore, it is expected that the matching accuracy should be relatively higher, particularly for a static time period (i.e., 5-min interval). However, for real-time application, the potential changes in traffic conditions would lead to dramatic decrease/increase in matching accuracy. Fig. 5

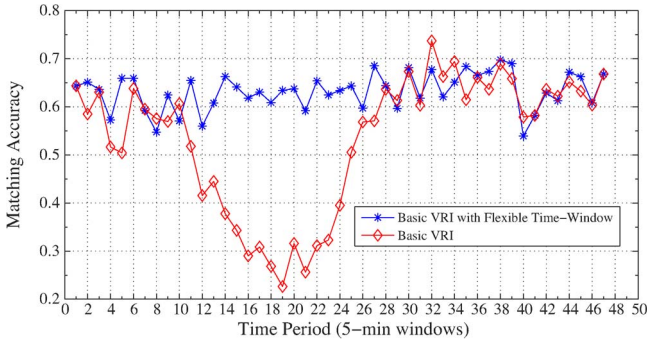


Fig. 5. Effectiveness of the self-adaptive time window.

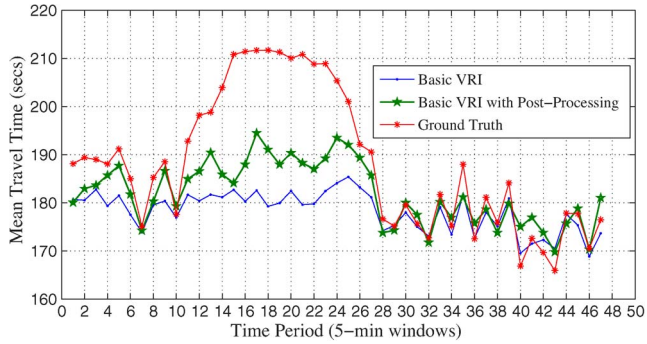


Fig. 6. Effectiveness of the postprocessing technique under a fixed time window.

shows the effectiveness of the basic VRI by employing the self-adaptive time window. As the traffic volume significantly increases during the second hour of the simulation experiment, the corresponding traffic condition changes from free-flow to congested. It is quite obvious that the fixed time window cannot handle this complicated situation (i.e., significant drop in matching accuracy from period 12 to 26), whereas the VRI system with a flexible time window can maintain a relatively stable matching accuracy (around 60% of matching accuracy).

On the other hand, given the fixed time window, a proper postprocessing technique (i.e., thresholding and stratified sampling) can still improve the model performance from the travel time estimation purpose. As shown in Fig. 6, the performance of the basic VRI significantly decays in the congested case due to the decrease in matching accuracy. However, it is worth noticing that the accuracy in mean travel time estimation improves a lot by imposing the postprocessing technique.

### C. Performance Evaluation Under Recurrent Traffic Congestion

To further evaluate the performance of the improved VRI system (i.e., with postprocessing and self-adaptive time window) under recurrent traffic congestion (due to exceeding traffic demand), the three-lane closed segment (between 08A and 10A) is chosen for the test site. The stochastic vehicle inputs of the VISSIM-based simulation model are defined as

$$Q = \begin{cases} 4000 \text{ veh/h,} & 0 \leq t \leq 60 \text{ min} \\ 7000 \text{ veh/h,} & 60 \leq t \leq 120 \text{ min} \\ 8000 \text{ veh/h,} & 120 \leq t \leq 180 \text{ min} \\ 4000 \text{ veh/h,} & 180 \leq t \leq 240 \text{ min.} \end{cases} \quad (29)$$

The vehicle inputs are chosen such that all the traffic states ranging from free-flow to congested can be activated. The freeway segment operates under the free-flow condition in the first stage (i.e., first hour). Congestion may be observed when the vehicle inputs switch to the second stage. Then, the traffic tends to a steady state of congestion during the following two hours. In the fourth stage, congestion dissolve will be observed, and the traffic will gradually be cleared from the freeway system. Table I shows descriptive statistics for the outputs from the VISSIM-based simulation model.

To validate the overall performance of the improved VRI system, we run the method 50 times based on the simulation outputs. For each run, the vehicle image is randomly selected from the database and assigned to the vehicle records generated from the simulation model. The root mean square error (RMSE) and the mean absolute percentage error (MAPE) are applied as performance indexes. The equation of the RMSE is given by

$$\text{RMSE} = \sqrt{\frac{1}{50} \sum_{s=1}^{50} \sum_{i=1}^I \frac{(\mu_{i(s)} - \mu_i^*)^2}{I}} \quad (30)$$

where  $\mu_{i(s)}$  is the estimate for the  $i$ th time period and the  $s$ th run,  $I$  indicates the total number of time periods, and  $\mu_i^*$  represents the  $i$ th ground truth data. The MAPE is calculated as

$$\text{MAPE} = \frac{1}{50 \times I} \sum_{s=1}^{50} \sum_{i=1}^I \left[ \left| \frac{\mu_{i(s)} - \mu_i^*}{\mu_i^*} \right| \times 100 \right]. \quad (31)$$

By simple calculation, the RMSE and the MAPE of the improved VRI system for a 5-min aggregation interval are 3.28 s and 1.0%, respectively, whereas the RMSE of the basic VRI is 14.61 s. It is observed that the improved VRI clearly outperforms the basic VRI. Fig. 7 shows the mean travel time estimates from one experiment. By integrating the average spot speed information (see Table I), interperiod adjusting can capture the traffic dynamics well, which could contribute to the following intraperiod adjusting (i.e., less intraperiod iteration steps).

### D. Performance Evaluation Under Bottleneck Effect

As one of the major causes for freeway traffic congestion, the freeway bottleneck can arise from many conditions, such as high merging and diverging demand at on/off-ramps and lane drops. In this part, we will evaluate the performance of the proposed method under the bottleneck effect. A 4.6-km-long three-lane freeway segment between 02A and 04A (see Fig. 4) is chosen as the test site. As shown in Fig. 8, one two-lane on-ramp (2 km away from the upstream station) and one two-lane off-ramp are distributed along this segment. We will ignore the off-ramp at this location since it does not affect the bottleneck area. The vehicle inputs at the upstream station are the same as (29), and we assume the following distribution of vehicle flows.

- 02A to 04A: 100%.
- Off-ramp: 15% of the vehicle flow will exit from the two-lane off-ramp.

TABLE I  
DESCRIPTIVE STATISTICS FROM SIMULATION OUTPUTS

Time: (0 min-240 min)	Simulation outputs				
	Vehicle Inputs (veh/h)	No. of small Vehicles	No. of long Vehicles	Upstream mean speed (km/h)	Downstream mean speed (km/h)
First hour	3982	2786	1196	<b>82.7</b>	<b>73.3</b>
Second hour	5964	4203	1761	<b>68.0</b>	<b>69.1</b>
Third hour	6214	4390	1824	<b>47.3</b>	<b>65.1</b>
Fourth hour	3934	2746	1188	<b>80.7</b>	<b>72.7</b>

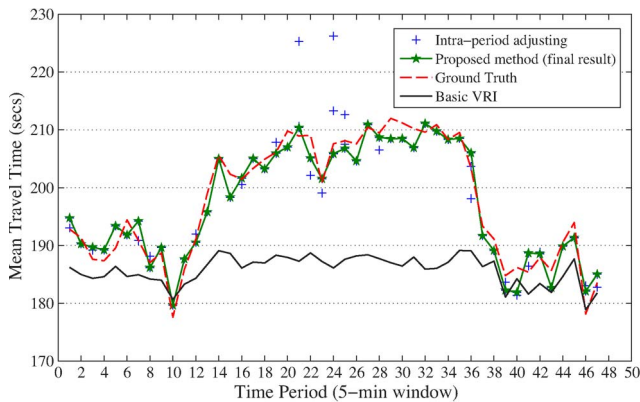


Fig. 7. Performance of the proposed method with exceeding traffic demand.

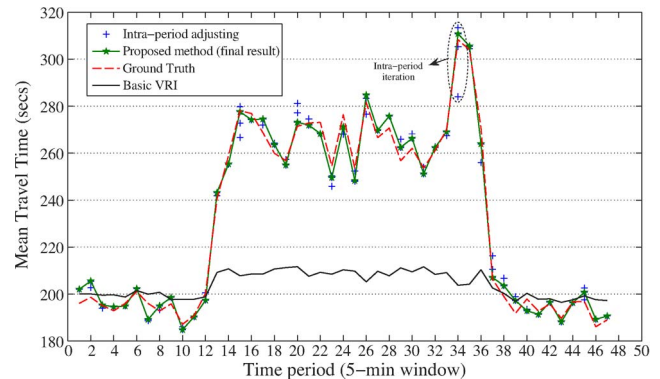


Fig. 9. Performance of the proposed method (on-ramp vehicle flow distribution: 25%).



Fig. 8. Merge and diverge along the freeway segment.

- On-ramp to the freeway segment: 25% of the vehicle flow will enter the freeway system through on-ramp (different flow distributions will be tested in the experiment).

With respect to the above simulation outputs, we run the proposed method 50 times. Fig. 9 shows the estimation results from one experiment. Compared with the basic VRI, the proposed method provides more reliable estimates of the mean travel time. In general, the bottleneck effect cannot be detected through the average speed at upstream and downstream stations, which means that interperiod adjusting cannot capture the traffic dynamics (congestion) well. Therefore, the num-

TABLE II  
PERFORMANCE OF THE PROPOSED METHOD WITH DIFFERENT VEHICLE FLOW DISTRIBUTIONS

On-ramp vehicle flow distribution (%)	Performance indices	
	RMSE (secs)	MAPE (%)
15%	3.62	1.3%
25%	5.50	1.9%
35%	5.54	1.8%
50%	9.42	2.8%

ber of intraperiod iteration steps would increase accordingly (see Fig. 9).

Table II also shows the performance of the improved VRI system under different vehicle distributions (i.e., on-ramp vehicle flow distribution). Since the test site is a freeway corridor with on/off-ramps, the vehicle arrives at the upstream station may not necessarily appear at downstream. In addition, some vehicles may enter this corridor through the on-ramp. Thus, it is expected that the matching accuracy of the proposed method is relatively lower. With the increase in the vehicle flow from on-ramp, the performance would gradually decay. However, it should be noted that the proposed method can still perform well against the bottleneck effect.

*E. Performance Evaluation Under Nonrecurrent Traffic Congestion*

As the nonrecurrent congestion is largely produced by traffic incidents, this research will investigate the performance of the proposed method under traffic incidents. The test site is also a three-lane closed segment (between 08A and 10A) and with the same vehicle inputs as (29). To mimic the situation of incident happening, a parking lot located at lane 1 (2 km away from the upstream station) is utilized to simulate the incident vehicle (see Fig. 10). When an incident happens (i.e., incident starts

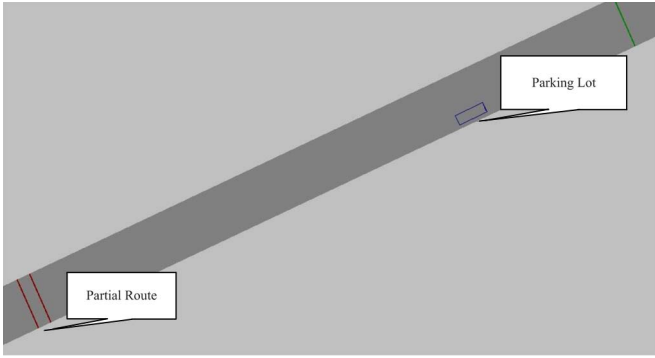


Fig. 10. Incident simulation.

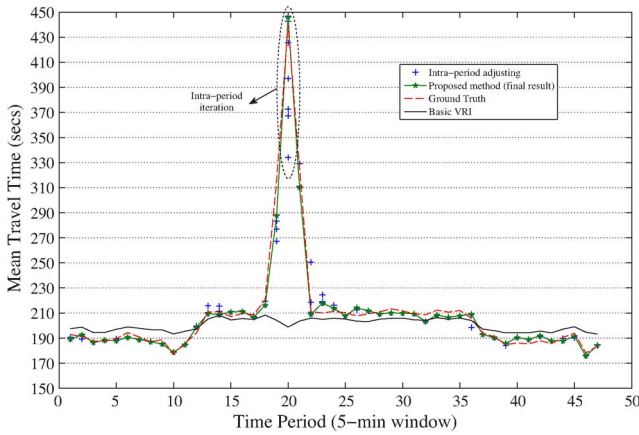


Fig. 11. Performance of the proposed method (incident duration: 10 min; starts from 90 min).

from 90 min), a vehicle would stop in the parking lot, and the partial route is activated to simulate the driving behavior under the incident condition.

The proposed algorithm is further tested with different incident durations (e.g., 10, 15, 20, and 30 min). Due to the unpredictability of the traffic incidents, interperiod adjusting cannot generate a suitable time window. Therefore, it is expected that the steps of intraperiod iteration would significantly increase, particularly when a traffic incident occurs. Fig. 11 shows the mean travel time estimates from one experiment when the incident duration is 10 min. It is observed that the mean travel time sharply increases during time period 20 (i.e., from 100 to 105 min). Hence, accordingly, the number of intraperiod iteration steps during this time period significantly increases. Fig. 12 also illustrates the adjustment of the time-window constraint for each iteration step. On the other hand, the basic VRI system cannot adapt well to the sudden changes in traffic condition when an incident happens (see Fig. 11). Due to the fixed time-window constraint, the matching accuracy of basic VRI drops to 0% during time period 20, which eventually leads to a totally unreliable estimate of the mean travel time.

Parallel to the previous experiments, we also run the method 50 times based on the simulation outputs for different incident durations (e.g., 10, 20, and 30 min). The detailed estimation results are shown in Table III. With the increase in incident durations, the RMSE and the MAPE increase as well. With the time propagation, it is also observed that the variance of

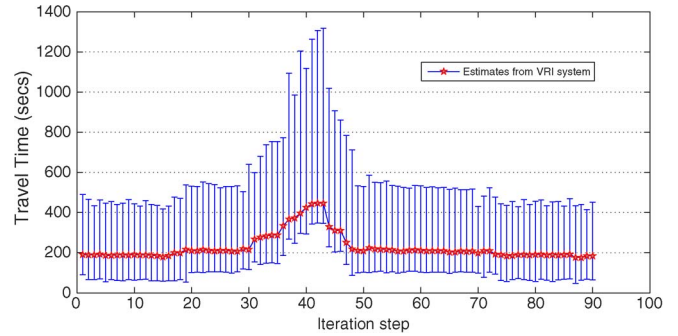


Fig. 12. Adjustment of the time-window constraint.

TABLE III  
PERFORMANCE OF THE PROPOSED METHOD WITH DIFFERENT INCIDENT DURATIONS

Incident durations (min) (%)	Performance indices	
	RMSE (secs)	MAPE (%)
10 min	<b>5.61</b>	1.5%
20 min	<b>22.41</b>	2.3%
30 min	<b>25.63</b>	2.8%

travel time dramatically increases (periods 21 and 22). The “abnormal” vehicle (seriously delayed by the incident at lane 1) and those normal vehicles may arrive at downstream during the same time period. In this case, it renders a heavy burden on the processing of the improved VRI system (e.g., larger time window, more candidate vehicles, and of course, low matching accuracy). Therefore, the results shown in Table III are reasonable.

VI. CONCLUSION AND FUTURE WORKS

This paper aims to develop an improved VRI system based on the authors’ previous work to estimate the real-time travel time under traffic demand and supply uncertainty. A self-adaptive time-window component is introduced into the basic VRI system to improve its adaptability against potential significant changes in traffic conditions. In addition, the associated postprocessing technique (i.e., thresholding based on the matching probability and stratified sampling based on the vehicle type) is employed to identify and rule out the erroneous travel time data. The proposed method is evaluated by conducting various representative simulation tests. Some performance indexes such as RMSE and MAPE are also introduced to quantify the performance of this method.

Further research will be focused on the real-world application of this proposed method. It is undeniable that the VIP systems are subject to the effects of inclement weather (e.g., rain and snow) and illumination changes. Under these circumstances, the quality of the video image will dramatically decrease and, hence, compromise the effectiveness of vehicle feature extraction. During evening hours, the vehicle may still be partially identified by detecting the vehicle headlight and taillight. However, the color information and vehicle type may not be obtained from the image. In this case, improving the external lighting condition at each station may be a promising way for vehicle feature extraction.

As validated by the simulated tests, the proposed VRI system for travel time estimation performs well under different scenarios (e.g., recurrent traffic congestion, freeway bottlenecks, and minor traffic accidents). However, it is noteworthy that the proposed method may not work well under extremely abnormal traffic conditions (e.g., severe traffic accident with longer incident duration). As explained in Section V-E, the longer incident duration would inevitably lead to a larger time window, low matching accuracy of the proposed VRI system, and hence an unreliable travel time estimator. Therefore, future efforts should be dedicated to overcome these drawbacks. As the lane blocking caused by incidents would produce a significant impact on the travel time experienced by the vehicles at different lanes, one possible way is then to perform stratified sampling based on the vehicle lane position.

#### REFERENCES

- [1] D. Ni and H. Wang, "Trajectory reconstruction for travel time estimation," *J. Intell. Transp. Syst.*, vol. 12, no. 3, pp. 113–125, Aug. 2008.
- [2] F. Soriguera and F. Robuste, "Requiem for freeway travel time estimation methods based on blind speed interpolations between point measurements," *IEEE Trans. Intell. Transp. Syst.*, vol. 12, no. 1, pp. 291–297, Mar. 2011.
- [3] H. B. Celikoglu, "Flow-based freeway travel-time estimation: A comparative evaluation within dynamic path loading," *IEEE Trans. Intell. Transp. Syst.*, vol. 14, no. 2, pp. 772–781, Jun. 2013.
- [4] C. Lindveld, R. Thijs, P. Bovy, and N. V. der Zijpp, "Evaluation of online travel time estimators and predictors," *Transp. Res. Rec.*, vol. 1719, no. 1, pp. 45–53, 2000.
- [5] R. Li, G. Rose, and M. Sarvi, "Evaluation of speed-based travel time estimation models," *J. Transp. Eng.*, vol. 132, no. 7, pp. 540–547, Jul. 2006.
- [6] S. M. Quayle, P. Koonce, D. DePencier, and D. M. Bullock, "Arterial performance measures with media access control readers: Portland, Oregon, pilot study," *Transp. Res. Rec.*, vol. 2192, pp. 185–193, Dec. 2010.
- [7] A. Hofleitner, R. Herring, P. Abbeel, and A. Bayen, "Learning the dynamics of arterial traffic from probe data using a dynamic Bayesian network," *IEEE Trans. Intell. Transp. Syst.*, vol. 13, no. 4, pp. 1679–1693, Dec. 2012.
- [8] S. Chang, L. Chen, Y. Chung, and S. Chen, "Automatic license plate recognition," *IEEE Trans. Intell. Transp. Syst.*, vol. 5, no. 1, pp. 42–53, Mar. 2004.
- [9] G. Rose, "Mobile phones as traffic probes: Practices, prospects and issues," *Transp. Rev.*, vol. 26, no. 3, pp. 275–291, May 2006.
- [10] C. Sun and S. G. Ritchie, "Individual vehicle speed estimation using single loop inductive waveforms," *J. Transp. Eng.*, vol. 125, no. 6, pp. 531–538, Nov./Dec. 1999.
- [11] B. Coifman, "Estimating travel times and vehicle trajectories on freeways using dual loop detectors," *Transp. Res. Part A*, vol. 36, no. 4, pp. 351–364, May 2002.
- [12] B. Coifman and S. Krishnamurthy, "Vehicle reidentification and travel time measurement across freeway junctions using the existing detector infrastructure," *Transp. Res. Part C*, vol. 15, no. 3, pp. 135–153, Jun. 2007.
- [13] S. Kamijo, T. Kawahara, and M. Sakauchi, "Vehicle sequence image matching for travel time measurement between intersections," in *Proc. IEEE Int. Conf. Syst., Man, Cybern.*, 2005, vol. 2, pp. 1359–1364.
- [14] C. C. Sun, G. S. Arr, R. P. Ramachandran, and S. G. Ritchie, "Vehicle reidentification using multidetector fusion," *IEEE Trans. Intell. Transp. Syst.*, vol. 5, no. 3, pp. 155–164, Sep. 2004.
- [15] D. P. Watling and M. J. Maher, "A statistical procedure for estimating a mean origin–destination matrix from a partial registration plate survey," *Transp. Res. Part B*, vol. 26, no. 3, pp. 171–193, Jun. 1992.
- [16] D. P. Watling, "Maximum likelihood estimation of an origin–destination matrix from a partial registration plate survey," *Transp. Res. Part B*, vol. 28, no. 4, pp. 289–314, Aug. 1994.
- [17] B. Coifman, "Vehicle re-identification and travel time measurement in real-time on freeways using existing loop detector infrastructure," *Transp. Res. Rec.*, vol. 1643, no. 1, pp. 181–191, 1998.
- [18] K. Kwong, R. Kavalier, R. Rajagopal, and P. Varaiya, "Arterial travel time estimation based on vehicle re-identification using wireless magnetic sensors," *Transp. Res. Part C*, vol. 17, no. 6, pp. 586–606, Dec. 2009.
- [19] K. Kwong, R. Kavalier, R. Rajagopal, and P. Varaiya, "Real-time measurement of link vehicle count and travel time in a road network," *IEEE Trans. Intell. Transp. Syst.*, vol. 11, no. 4, pp. 814–825, Dec. 2010.
- [20] A. Sumalee, J. Wang, K. Jedwana, and S. Suwansawat, "Probabilistic fusion of vehicle features for re-identification and travel time estimation using video image data," *Transp. Res. Rec.*, vol. 2308, pp. 73–82, 2012.
- [21] C. Mallikarjuna, A. Phanindra, and K. R. Rao, "Traffic data collection under mixed traffic conditions using video image processing," *J. Transp. Eng.*, vol. 135, no. 4, pp. 174–182, Apr. 2009.
- [22] L. A. Klein, M. K. Mills, and D. R. P. Gibson, *Traffic Detector Handbook*, 3rd ed. Washington, DC, USA: Federal Highway Administration, 2006.
- [23] W. Lin and D. Tong, "Vehicle re-identification with dynamic time windows for vehicle passage time estimation," *IEEE Trans. Intell. Transp. Syst.*, vol. 12, no. 4, pp. 1057–1063, Dec. 2011.
- [24] M. Ndoye, V. F. Totten, J. V. Krogmeier, and D. M. Bullock, "Sensing and signal processing for vehicle reidentification and travel time estimation," *IEEE Trans. Intell. Transp. Syst.*, vol. 12, no. 1, pp. 119–131, Mar. 2011.
- [25] A. T. G. Thiang and R. Lim, "Type of vehicle recognition using template matching method," in *Proc. Int. Conf. Electr., Electron., Commun., Inf.*, 2001, pp. 1–5.
- [26] A. Bhattacharyya, "On a measure of divergence between two statistical populations defined by their probability distributions," *Bull. Calcutta Math. Soc.*, vol. 35, no. 1, pp. 99–109, 1943.
- [27] B. R. Hellinga and L. Fu, "Reducing bias in probe-based arterial link travel time estimates," *Transp. Res. Part C*, vol. 10, no. 4, pp. 257–273, Aug. 2002.
- [28] M. C. Tan, S. C. Wong, J. M. Xu, Z. R. Guan, and P. Zhang, "An aggregation approach to short-term traffic flow prediction," *IEEE Trans. Intell. Transp. Syst.*, vol. 10, no. 1, pp. 60–69, Mar. 2009.
- [29] Q. Ye, W. Y. Szeto, and S. C. Wong, "Short-term traffic speed forecasting based on data recorded at irregular intervals," *IEEE Trans. Intell. Transp. Syst.*, vol. 13, no. 4, pp. 1727–1737, Dec. 2012.



**Jiankai Wang** received the B.S. and M.S. degrees in mathematics, with a focus on operations research, applied optimization, and image reconstruction, from Nanjing University, Nanjing, China, in 2007 and 2010, respectively. He is currently working toward the Ph.D. degree in transportation engineering in the Department of Civil and Environmental Engineering, The Hong Kong Polytechnic University, Kowloon, Hong Kong.

His research interests include image processing, traffic surveillance and management, and optimization in intelligent transportation systems.



**Nakorn Indra-Payoong** received the Ph.D. degree in computing from the University of Leeds, Leeds, U.K.

He is currently an Associate Professor of logistics and supply chain management with the Faculty of Logistics, Burapha University, Bangkok, Thailand. His research interests include large-scale network optimization and intelligent transport systems.



**Agachai Sumalee** received the B.Eng. degree in civil engineering from King Mongkut's Institute of Technology Ladkrabang, Bangkok, Thailand, in 1999 and the M.Sc.(Eng.) and Ph.D. degrees in transportation planning and engineering from the University of Leeds, Leeds, U.K., in 2000 and 2004, respectively.

He is an Associate Professor with the Department of Civil and Environmental Engineering, The Hong Kong Polytechnic University, Kowloon, Hong Kong. He has published more than 60 research papers in top peer-reviewed journals. His research interests

include transit planning, intelligent transport systems, network modeling and optimization, and transport economics.

Dr. Sumalee is the Editor-in-Chief of *Transportmetrica B: Transport Dynamics*, the Editor of *Transport Policy*, an Associate Editor of *Networks and Spatial Economics*, and an Editorial Board Member of several prestigious journals. He has received several prizes and awards for his research works.



**Sakda Panwai** received the B.Sc.Id.Ed. degree in civil engineering (first-class honor) from King Mongkut's Institute of Technology Thonburi, Bangkok, Thailand, in 1996; the M.E. degree in transportation engineering from the Asian Institute of Technology, Pathumthani, Thailand, in 1998; and the Ph.D. degree from The University of Queensland, Brisbane, Australia, in 2007.

For over 15 years, he has been with the Expressway Authority of Thailand (EXAT), Bangkok, where he is responsible for conducting feasibility studies,

highway design, research studies (e.g., traffic impact analysis and traffic studies), and the development of intelligent transportation system (ITS) applications (e.g., incident detection system, travel time estimation, and road and vehicle emission including the urban heat island study). His research interests include ITS applications, smart infrastructure, and advanced ITS system modeling using a traffic simulation technique.

Dr. Panwai received an EXAT Scholarship for his Master's degree in 1996, an International Road Federation Fellowship award in 2002/2003, a Royal Government (RTG) Scholarship for his doctoral study in 2003, and the European Marie Curie Award for attending a training course in Berlin, Germany, in 2005. In 2011, he was invited to Hiroshima University for a research fellowship program.